

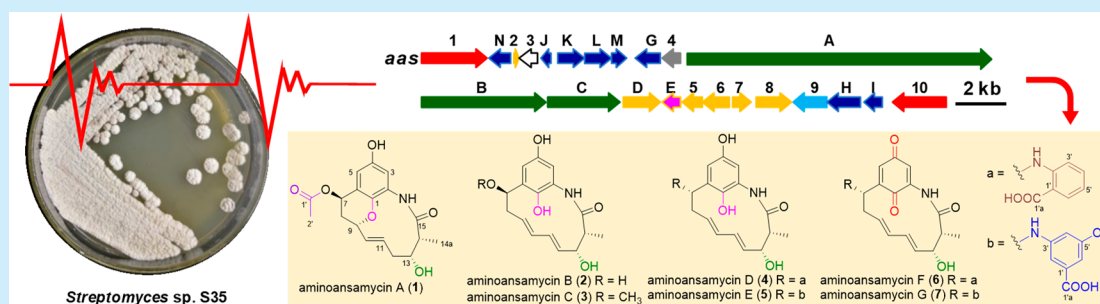
Targeted Discovery of Pentaketide Ansamycin Aminoansamycins A–G

Feifei Wei,^{†,§} Zishen Wang,^{†,§} Chunhua Lu,^{‡,§} Yaoyao Li,^{‡,§} Jing Zhu,[†] Haoxin Wang,^{*,†,§} and Yuemao Shen^{†,‡,§}

[†]State Key Laboratory of Microbial Technology, Shandong University, Qingdao, Shandong 266237, P. R. China

[‡]Key Laboratory of Chemical Biology (Ministry of Education), School of Pharmaceutical Sciences, Shandong University, Jinan, Shandong 250012, P. R. China

Supporting Information



ABSTRACT: Ansamycins are a class of macrolactams with diverse bioactivities, characterized by the unique 3-amino-5-hydroxybenzoic acid moiety. In this study, the ansamycin gene cluster *aas* in *Streptomyces* sp. S35 was activated by the constitutive coexpression of two pathway-specific regulator genes *aas1* and *aas10*, and seven novel pentaketide ansamycin aminoansamycins A–G (1–7) were identified. Compound 4 with better antiproliferative activity indicated that the anthranilate analogues are probably promising building blocks for the production of unnatural ansamycins with improved activity.

Ansamycins are a family of macrolactams that are assembled by type-I polyketide synthases (PKSs) using unique 3-amino-5-hydroxybenzoic acid (AHBA) as the starter unit and released by amide synthase.¹ Representative members of this family include the first-line antituberculous drug rifamycin (undecaketide),² the cytotoxic component of the antibody–drug conjugate Kadcyla maytansinoid (octaketide),³ and the first Hsp90 inhibitor geldanamycin (octaketide).⁴ According to the extension modules presented in the PKSs, known ansamycins are classified into six groups, including pentaketide, heptaketide, octaketide, nonaketide, heptaketide, undecaketide, and tetradecaketide.^{5,6} To date, nearly 300 ansamycins have been reported, of which only 20 pentaketide ansamycins with four different scaffolds have been identified, including tetrapetalones,^{7–9} cebulactams,¹⁰ juanlimycins,¹¹ and microansamycins¹² (Figure S1). Two of the four pentaketide scaffolds, juanlimycins and microansamycins, were previously discovered by our group.^{11,12} During our search for new ansamycins, we identified another novel pentaketide ansamycin gene cluster. Herein, we report the identification of the *aas* gene cluster in *Streptomyces* sp. S35 and the structural elucidation of seven novel pentaketide ansamycins with nonproteinogenic amino acid side chains, aminoansamycins A–G (1–7). The activity tests showed that aminoansamycins A–E (1–5) have potent activity against cancer cell lines.

Streptomyces sp. S35 was isolated from the soil collected from Kunming, Yunnan, China and identified as an AHBA-synthase-positive strain by polymerase chain reaction (PCR) screening using the primers that target AHBA synthase genes, as previously reported.¹³ Bioinformatics analysis of the genomic sequence of *Streptomyces* sp. S35 was carried out by using the standard antiSMASH 4.0 algorithm,¹⁴ and a pentaketide ansamycin biosynthetic gene cluster (*aas*) (Figure 1a, Table S2, GenBank no. MH045679) was found. It contains three type-I PKS genes (*aasA–C*), an amide synthase gene (*aasE*), and eight AHBA biosynthetic genes (*aasG–N*). In addition, the cluster contains genes coding for post-PKS tailoring enzymes, transcriptional regulators, a putative transporter, and a type-II thioesterase (TE). The polyketide backbone of the product was proposed to be AHBA–C₂–C₂–C₂–C₃, which is different from the four known pentaketide ansamycin skeletons (Figure S1) and predicted to be novel. However, no ansamycins were isolated from the *Streptomyces* sp. S35 wild type (WT) by scale-up fermentation (10 L of YMG agar medium).

To improve the production of the metabolites encoded by the *aas* gene cluster, we carried out the constitutive expression of the pathway-specific LAL (large ATP-binding regulators of

Received: August 8, 2019

Published: September 16, 2019

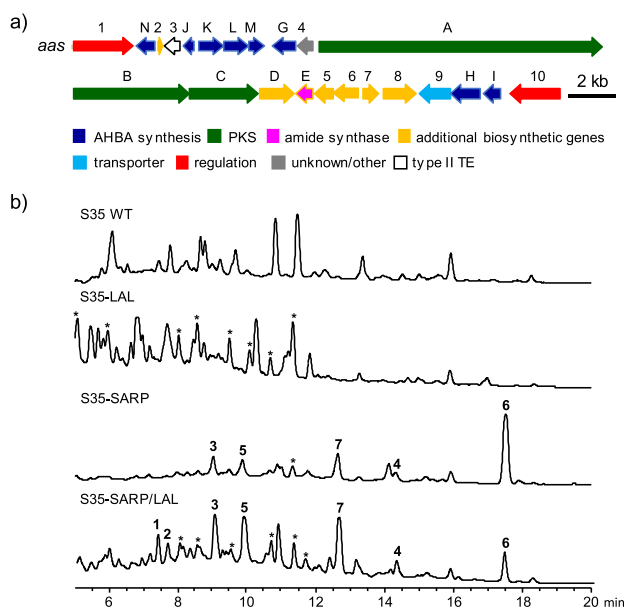


Figure 1. (a) Genetic organization of the *aas* gene cluster in *Streptomyces* sp. S35. (b) HPLC profiles of the metabolites of the control strain S35 WT, the LAL gene (*aas1*) overexpressed strain S35-LAL, the SARP gene (*aas10*) overexpressed strain S35-SARP, and the SARP gene and LAL gene overexpressed strain S35-SARP/LAL. The seven characterized aminoansamycins (1–7) that were not present in S35 WT are indicated. The “*” symbol denotes uncharacterized aminoansamycin analogues, which were identified by diode array UV comparison with compounds 1–7 (Figure S3).

the LuxR family) and SARP (*Streptomyces* antibiotic regulatory protein family) regulator genes *aas1* and *aas10* as previously reported.^{12,15–17} *aas1* and *aas10* were individually or co-overexpressed in the strain S35 WT to give three recombinant strains S35-LAL, S35-SARP, and S35-SARP/LAL (Figure S2). By applying a comparative HPLC profiling approach, several peaks were identified in strains S35-LAL, S35-SARP, and S35-SARP/LAL that were absent in the control strain S35 WT (Figure 1b). In addition, strain S35-SARP/LAL contained almost all of the extra peaks shown in S35-SARP and part of those in S35-LAL. Therefore, we set out a solid-state fermentation (40 L) of strain S35-SARP/LAL with ISP3 medium for 10 days at 28 °C and obtained the MeOH extract, which was subjected to medium-pressure liquid chromatography (MPLC), Sephadex LH-20 liquid chromatography medium, a silica gel column chromatogram, and high-performance liquid chromatography (HPLC) to yield compounds 1–7 (Figure 2).

Aminoansamycin A (**1**) was obtained as a colorless needle crystal. The molecular formula of **1** was established as C₁₈H₂₁NO₆ based on the high-resolution electrospray ionization mass spectrometry (HR ESIMS) *m/z* 348.1442 [M + H]⁺ (calcd for C₁₈H₂₂NO₆⁺, 348.1442) (Figure S10). The ¹H and ¹³C nuclear magnetic resonance (NMR) and heteronuclear single quantum coherence (HSQC) spectrum revealed 18 carbon signals, corresponding to two CH₃, two CH₂, eight CH, and six quaternary C atoms. A tetrasubstituted *p*-hydroquinone moiety was suggested by the heteronuclear multiple bond correlation (HMBC) correlations of H3 (δ_H 7.62) to C1 (δ_C 143.4), C2 (δ_C 132.4), C4 (δ_C 154.3), and C5 (δ_C 114.2) and H5 (δ_H 7.31) to C1, C3 (δ_C 116.1), C4, and C7 (δ_C 69.2). A fragment from C7 to C15 was established

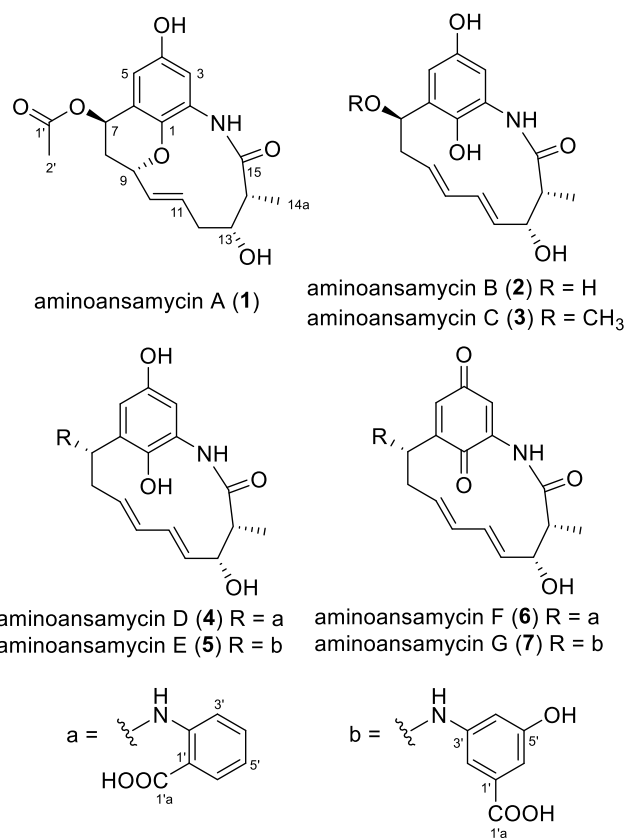


Figure 2. Chemical structures of aminoansamycins A–G (1–7).

based on the ¹H–¹H COSY correlations of H7–H14a and the HMBC correlations of H14a to C13, C14, and C15 (Table S4). The HMBC correlations of H2' and H7 to C1' confirmed the presence of an acetoxy group at C7. Then, these two fragments were connected based on the HMBC correlations of H7 to C1, C5, and C6, and NH (δ_H 10.38) to C1, C3, and C15 (δ_C 178.6). In addition, the HMBC correlation of H9 (δ_H 5.18) to C1 revealed the existence of an ether linkage between C-9 and C1. The large coupling constant (*J* = 14.8 Hz) between H10 and H11 led to the assignment of the 10*E* configuration for **1**. To determine the absolute configuration of **1**, a single-crystal X-ray diffraction analysis with Cu Kα radiation was performed (CCDC 1821760, Figure 3). Accordingly, the absolute stereochemistry of **1** was determined to be 7*R*,9*S*,13*R*,14*R*.

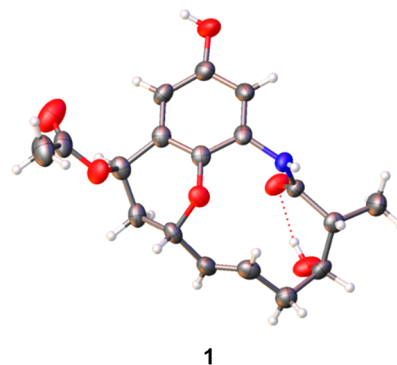


Figure 3. Single-crystal X-ray structure of **1**.

Aminoansamycin B (**2**) was obtained as a yellow powder. Its molecular formula was established to be $C_{16}H_{19}NO_5$ on the basis of the HR ESIMS m/z 306.1332 $[M + H]^+$ (calcd for $C_{16}H_{20}NO_5^+$, 306.1336) (Figure S17). The interpretation of the HR ESIMS and NMR data indicated that **2** had the same ansa skeleton as that of **1** (Table S5). The apparent difference between **2** and **1** is the presence of two carbon–carbon double bonds (Δ^9 , Δ^{11}) in the ansa chain and the absence of an acetyl group at C7 in **2**. The large coupling constants ($J > 15.0$ Hz) between H9/H10 and H11/H12 suggested 9E and 11E configurations in **2**.

Aminoansamycin C (**3**) was obtained as a yellow powder. The NMR data of **3** were similar to those of **2**, except that C7 was substituted by a hydroxymethyl group deduced from the HMBC correlation of C1' (δ_H 3.48 and δ_C 57.7) to C7 (Table S6), which was further supported by the HR ESIMS at m/z 320.1492 $[M + H]^+$ (calcd for $C_{17}H_{22}NO_5^+$, 320.1492) (Figure S24).

The analysis of the NMR spectra of aminoansamycin D (**4**) and aminoansamycin E (**5**) revealed that they bear the same substructure as **2** (Tables S7 and S8). In addition, the large coupling constant ($J > 15.0$ Hz) between H9/10 and H11/12 confirmed 9E and 11E configurations, as in **2**. Compound **4** differs from **2** in the presence of an anthranilate residue, which was established by the 1H – 1H COSY correlations of H3'–H6', the HMBC correlations of H3' to C1' and C5' and H6' to C1'a, C2', and C4', and the HR ESIMS at m/z 425.1709 $[M + H]^+$ (calcd for $C_{23}H_{25}N_2O_6^+$, 425.1707) of **4** (Figure S31). The anthranilate residue was attached to C7 via an amino group supported by the HMBC correlation of H7 to C2'. The relative configuration of C7 was determined on the basis of the nuclear Overhauser effect (NOE) correlations of NH7/H9/H11, H7/H5/H8 β /H10, and H12/H14, which is opposite to that in **1**. The difference between **5** and **4** was that the anthranilate residue in **4** was replaced by an AHBA residue in **5**. The AHBA fragment in **5** was established by the presence of the three singlet protons in the 1H NMR spectra and their related HMBC correlations (Table S8), which was further confirmed by the ion peak at m/z 441.1656 $[M + H]^+$ (calcd for $C_{23}H_{25}N_2O_7^+$, 441.1656) of **5** (Figure S38). The AHBA residue was connected to C7, determined by the HMBC correlation of H7 to C3'.

The molecular formula of aminoansamycin F (**6**) and aminoansamycin G (**7**) was determined to be $C_{23}H_{22}N_2O_6^+$ and $C_{23}H_{22}N_2O_7^+$ by the HR ESIMS at 423.1553 $[M + H]^+$ and 439.1503 $[M + H]^+$, respectively (Figures S45 and S52). By comparing the NMR spectra of **6** and **4**, compound **6** was identified as an analogue of **4** with a *p*-benzoquinone moiety rather than a *p*-hydroquinone moiety (Table S9). Compound **7** is distinguished from **6** by the presence of an AHBA residue instead of an anthranilate residue (Table S10).

The cytotoxicity of compounds **1**–**7** was evaluated by an SRB assay (sulforhodamine B) using VP16 as a positive control. Compounds **2**–**6** showed potent antiproliferative activities against HeLa, PC-3, HTC116, and SW480 cell lines (Table 1). Interestingly, compound **4** showed higher activity than the others, indicating that the anthranilate residue and phenolic hydroxyl groups are probably crucial for the activity.

The biosynthetic route of aminoansamycins was proposed (Scheme 1). The PKS AasA–C is responsible for the assembly of the polyketide skeleton by employing AHBA as the starter unit and three malonyl–CoAs and one methylmalonyl–CoA as the extenders. Sequence analysis revealed that AasD is

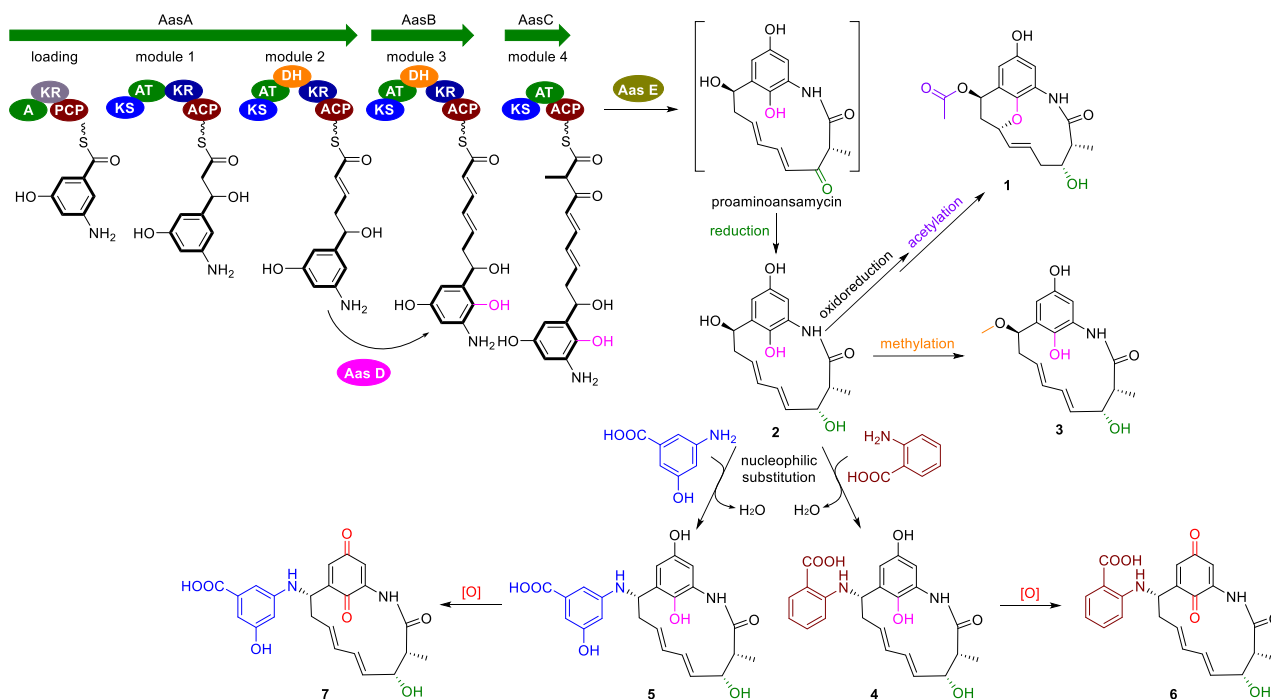
Table 1. Cytotoxicity of Compounds 1–7 against Test Cell Lines

| compd | IC ₅₀ (μ M) | | | |
|----------|-----------------------------|------|--------|-------|
| | HeLa | PC3 | HCT116 | SW480 |
| 1 | >50 | >50 | >50 | >50 |
| 2 | 21.2 | 27.8 | 31.2 | 42.4 |
| 3 | 23.7 | 16.9 | 27.9 | 32.3 |
| 4 | 7.9 | 9.1 | 10.1 | 17.3 |
| 5 | 17.9 | 35.6 | 22.8 | >50 |
| 6 | 31.2 | 47.9 | >50 | >50 |
| 7 | >50 | >50 | >50 | >50 |
| VP-16 | 0.31 | 0.61 | 3.6 | 3.1 |

similar to the hydroxylase Nam7 (53.1%) in the neoansamycin gene cluster, which is involved in the hydroxylation of AHBA.¹⁸ Then, the proposed proaminoansamycin was cyclized and released from PKSs by the amide synthase AasE. The intermediate was reduced to give **2** and subsequently modified by oxidoreduction and acetylation to afford **1**. Aas6 is homologous to acyltransferase, which may be involved in the acetylation reaction. Methylation at C7–OH converted **2** to **3**. However, there is not a candidate for methyltransferase present in the *aas* gene cluster or its flanking regions. The addition of the methyl group at C7–OH could use a methyltransferase in the other region of the chromosome. A nucleophilic substitution reaction takes place during the biological conversion of **2** to **4** and **5**, which were further oxidized to afford **6** and **7**. Aas5 is homologous to the SDR (short-chain dehydrogenase/reductase) family oxidoreductase, and Aas8 is homologous to the FAD-dependent oxidoreductase. These two enzymes may be involved in the redox modifications. One thing to be noted is that the order of the addition of the amino acid residues and the oxidation of the *p*-hydroquinone moiety might be reversed. Because compounds **4**–**7** are not epimers, the attachment of the nonproteinogenic amino acids likely goes through a S_N2-type nucleophilic substitution, which is facilitated by the benzylic position of C7–OH. This means that C7 should have the opposite configuration of **2**, which is consistent with the structure of **4**. Similar S_N2-type reactions have been reported for chorismate-utilizing enzymes.¹⁹ The installation of an anthranilate or an AHBA unit on ansamycins is rare, and the only reported ones are the macrodilactam juanlimycins.¹¹

In summary, we have identified a cryptic ansamycin gene cluster through genome mining and successfully activated it by co-overexpression of the LuxR family regulator Aas1 and the SARP family regulator Aas10. As a result, seven novel pentaketide ansamycin aminoansamycins A–G (**1**–**7**) were identified, characterized by the nonproteinogenic amino acid side chains, an anthranilate, or an AHBA unit, covalently connected to the ansa chain via a C–N bond. In addition, compounds **2**–**6** have moderate antiproliferative activity, and **4** showed three times higher activity than **2**, indicating that the anthranilate group is important for the activity. Therefore, the elucidation of the mechanism for the installation of this functionality in the following research may facilitate the bioengineering of novel ansamycins with improved bioactivity. Finally, the discovery of aminoansamycins emphasizes again that the constitutive expression of the pathway-specific regulator is an efficient approach for awakening “silent” ansamycin gene clusters.

Scheme 1. Proposed Biosynthetic Pathway of Aminoansamycins



■ ASSOCIATED CONTENT

Supporting Information

The Supporting Information is available free of charge on the ACS Publications website at DOI: 10.1021/acs.orglett.9b02804.

Details of experimental procedures, metabolite production and isolation, and spectroscopic data of compounds 1–7 (PDF)

Accession Codes

CCDC 1821760 contains the supplementary crystallographic data for this paper. These data can be obtained free of charge via www.ccdc.cam.ac.uk/data_request/cif, or by emailing data_request@ccdc.cam.ac.uk, or by contacting The Cambridge Crystallographic Data Centre, 12 Union Road, Cambridge CB2 1EZ, UK; fax: + 44 1223 336033.

■ AUTHOR INFORMATION

Corresponding Author

*E-mail: wanghaoxin@sdu.edu.cn

ORCID

Chunhua Lu: 0000-0002-3261-1020

Yaoyao Li: 0000-0002-8762-9615

Haixin Wang: 0000-0002-1779-0286

Yuemao Shen: 0000-0002-3881-0135

Author Contributions

[§]F.W. and Z.W. contributed equally to this work.

Notes

The authors declare no competing financial interest.

■ ACKNOWLEDGMENTS

We thank Dr. Liangcheng Du for insightful discussions. This study was funded by the National Natural Science Foundation of China (31570039, 81530091, 81673317) and the Program

for Changjiang Scholars and Innovative Research Team in University (IRT_17R68).

■ REFERENCES

- (1) Floss, H. G.; Yu, T.; Arakawa, K. The biosynthesis of 3-amino-5-hydroxybenzoic acid (AHBA), the precursor of mC₇N units in ansamycin and mitomycin antibiotics: a review. *J. Antibiot.* **2011**, *64*, 35–44.
- (2) Maggi, N.; Pasqualucci, C. R.; Ballotta, R.; Sensi, P. Rifampicin: a new orally active rifamycin. *Chemotherapy* **1966**, *11*, 285–292.
- (3) Cassady, J. M.; Chan, K. K.; Floss, H. G.; Leistner, E. Recent developments in the maytansinoid antitumor agents. *Chem. Pharm. Bull.* **2004**, *52*, 1–26.
- (4) Whitesell, L.; Mimnaugh, E. G.; De Costa, B.; Myers, C. E.; Neckers, L. M. Inhibition of heat shock protein Hsp90-pp60v-src heteroprotein complex formation by benzoquinone ansamycins: essential role for stress proteins in oncogenic transformation. *Proc. Natl. Acad. Sci. U. S. A.* **1994**, *91*, 8324–8328.
- (5) Floss, H. G. Natural products derived from unusual variants of the shikimate pathway. *Nat. Prod. Rep.* **1997**, *14*, 433–452.
- (6) Kang, Q.; Shen, Y.; Bai, L. Biosynthesis of 3,5-AHBA-derived natural products. *Nat. Prod. Rep.* **2012**, *29*, 243–263.
- (7) Komoda, T.; Akasaka, K.; Hirota, A. Ansaetherone, a new radical scavenger from *Streptomyces* sp. *Biosci., Biotechnol., Biochem.* **2008**, *72*, 2392–2397.
- (8) Komoda, T.; Yoshida, K.; Abe, N.; Sugiyama, Y.; Imachi, M.; Hirota, H.; Koshino, H.; Hirota, A. Tetrapetalone A, a novel lipoxygenase inhibitor from *Streptomyces* sp. *Biosci., Biotechnol., Biochem.* **2004**, *68*, 104–111.
- (9) Komoda, T.; Kishi, M.; Abe, N.; Sugiyama, Y.; Hirota, A. Novel lipoxygenase inhibitors, tetrapetalone B, C, and D from *Streptomyces* sp. *Biosci., Biotechnol., Biochem.* **2004**, *68*, 903–908.
- (10) Pimentel-Elardo, S. M.; Gulder, T. A. M.; Hentschel, U.; Bringmann, G. Cebulactams A1 and A2, new macrolactams isolated from *Saccharopolyspora cebuensis*, the first obligate marine strain of the genus *Saccharopolyspora*. *Tetrahedron Lett.* **2008**, *49*, 6889–6892.
- (11) Zhang, J.; Qian, Z.; Wu, X.; Ding, Y.; Li, J.; Lu, C.; Shen, Y. Juanlimycins A and B, ansamycin macrodilactams from *Streptomyces* sp. *Org. Lett.* **2014**, *16*, 2752–2755.

(12) Wang, J.; Li, W.; Wang, H.; Lu, C. Pentaketide ansamycin microansamycins A-I from *micromonospora* sp. reveal diverse post-PKS modifications. *Org. Lett.* **2018**, *20*, 1058–1061.

(13) Wang, H.; Chen, Y.; Ge, L.; Fang, T.; Meng, J.; Liu, Z.; Fang, X.; Ni, S.; Lin, C.; Wu, Y.; Wang, M.; Shi, N.; He, H.; Hong, K.; Shen, Y. PCR screening reveals considerable unexploited biosynthetic potential of ansamycins and a mysterious family of AHBA-containing natural products in actinomycetes. *J. Appl. Microbiol.* **2013**, *115*, 77–85.

(14) Blin, K.; Wolf, T.; Chevrette, M. G.; Lu, X.; Schwalen, C. J.; Kautsar, S. A.; Suarez Duran, H. G.; de los Santos, E. L. C.; Kim, H. U.; Nave, M.; Dickschat, J. S.; Mitchell, D. A.; Shelest, E.; Breitling, R.; Takano, E.; Lee, S. Y.; Weber, T.; Medema, M. H. antiSMASH 4.0-improvements in chemistry prediction and gene cluster boundary identification. *Nucleic Acids Res.* **2017**, *45*, W36–W41.

(15) Zhao, G.; Li, S.; Guo, Z.; Sun, M.; Lu, C. Overexpression of *div8* increases the production and diversity of divergolides in *Streptomyces* sp. W112. *RSC Adv.* **2015**, *5*, 98209–98214.

(16) Xie, C.; Deng, J.; Wang, H. Identification of AstG1, A LAL family regulator that positively controls ansatrienin production in *Streptomyces* sp. XZQH13. *Curr. Microbiol.* **2015**, *70*, 859–864.

(17) Li, S.; Li, Y.; Lu, C.; Zhang, J.; Zhu, J.; Wang, H.; Shen, Y. Activating a cryptic ansamycin biosynthetic gene cluster to produce three new naphthalenic octaketide ansamycins with *n*-pentyl and *n*-butyl side chains. *Org. Lett.* **2015**, *17*, 3706–3709.

(18) Zhang, J.; Li, S.; Wu, X.; Guo, Z.; Lu, C.; Shen, Y. Nam7 hydroxylase is responsible for the formation of the naphthalenic ring in the biosynthesis of neoansamycins. *Org. Lett.* **2017**, *19*, 2442–2445.

(19) He, Z.; Stigers Lavoie, K. D.; Bartlett, P. A.; Toney, M. D. Conservation of mechanism in three chorismate-utilizing enzymes. *J. Am. Chem. Soc.* **2004**, *126*, 2378–2385.